Angewandte Chemie

Eine Zeitschrift der Gesellschaft Deutscher Chemiker

Supporting Information

69451 Weinheim, Germany

Conformational Control of Integrin-Subtype Selectivity in *iso*DGR Peptide Motifs: A Biological Switch**

*Andreas O. Frank, Elke Otto, Carlos Mas-Moruno, Herbert B. Schiller, Luciana Marinelli, Sandro Cosconati, Alexander Bochen, Dörte Vossmeyer, Grit Zahn, Roland Stragies, Ettore Novellino, and Horst Kessler**

anie_201004363_sm_miscellaneous_information.pdf

1. Full citation list

[6] S. Takahashi, M. Leiss, M. Moser, T. Ohashi, T. Kitao, D. Heckmann, A. Pfeifer, H. Kessler, J. Takagi, H. P. Erickson, R. Fässler, *J. Cell Biol.* **2007**, *178*, 167-178.

[26] R. Stupp, M. E. Hegi, B. Neyns, R. Goldbrunner, U. Schlegel, P. M. Clement, G. G. Grabenbauer, A. F. Ochsenbein, M. Simon, P. Y. Dietrich, T. Pietsch, C. Hicking, J. C. Tonn, A. C. Diserens, A. Pica, M. Hermisson, S. Krueger, M. Picard, M. Weller, *J. Clin. Oncol.* **2010**, *28*, 2712-2718.

[28] F. Curnis, A. Cattaneo, R. Longhi, A. Sacchi, A. M. Gasparri, F. Pastorino, P. Di Matteo, C. Traversari, A. Bachi, M. Ponzoni, G. P. Rizzardi, A. Corti, *J. Biol. Chem.* **2010**, *285*, 9114-9123.

2. Molecular structure of fibronectin

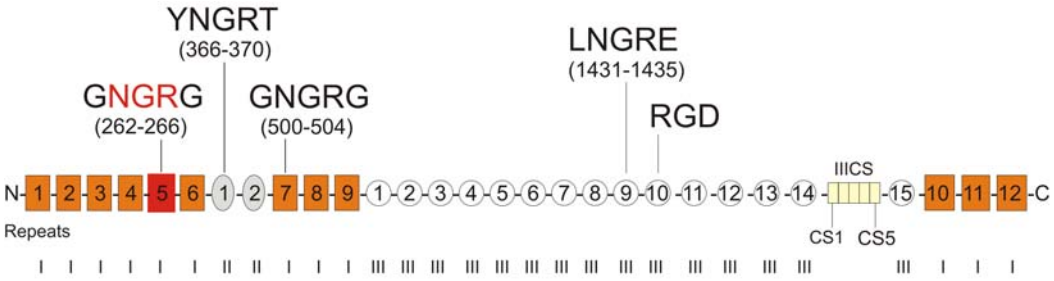

Figure SI_1: The modular structure of the extracellular matrix protein fibronectin. Even when the essential RGD recognition motif in domain III-10 (grey circle) is mutated to RGE, the protein still binds to αvβ3 and α5β1 integrin receptors. Previous studies revealed that this unexpected observation can be attributed to a rearrangement of the NGR amino acid sequence in domain I-5 (grey rectangle) into *iso*DGR. The NGR motif is also located at three further positions. The deamidation of asparagine, usually regarded as a process of protein degradation, results in an activation of fibronectin.

3. Synthesis of peptides

3.1 Materials and methods

Tritylchloride polystyrene (TCP) resin (0.94 mmol/g) was purchased from *PepChem* (Tübingen Germany). Coupling reagents and amino acid derivatives were purchased from *Merck Biosciences* (Läufelfingen, Switzerland), *Perseptive Biosystems GmbH* (Hambourg, Germany) and *Neosystem* (Strasbourg, France). All other reagents and solvents were purchased from *Merck* (Darmstadt, Germany), *Aldrich* (Steinheim, Germany) and *Fluka* (Neu-Ulm, Germany) and were used as received. Standard syringe techniques were applied for transferring dry solvents. Reactions on solid support were performed in filter columns (2 mL) from *Abimed*.
Analytical and preparative **HPLC** was performed on A) *Amersham Pharmacia Biotech*: Äkta Basic 10F; Pump system P-900; Detector UV-900; Driver software Unicorn, vers. 3.00; Column material: ODS-A C_{18} (120 Å, 5 µm, 250 mm x 4.6 mm); B) *Amersham Pharmacia Biotech:* Äkta Basic 100F; Pump system P-900; Detector UV-900, Driver software Unicorn vers. 3.00; Column material ODS-A C_{18} (120 Å, 10 µm, 250 mm x 20 mm). **ESI mass spectra** were recorded on a *Finnigan* LCQ combined with an HPLC-system *Hewlett Packard* HP1100 (Column material: Omnicrom YMC ODS-A C_{18} (120 Å, 3 µm, 125 mm x 2 mm). **NMR** spectra were recorded on *Bruker* AC250 and DMX500 using DMSO-d_6 as solvent and internal standard. Assignment was performed using different 2D-experiments such as TOCSY, HMQC-COSY. All yields are not optimized.

3.2 General procedure

Loading of TCP resin

Peptide synthesis was carried out using TCP resin (0.94 mmol/g) following standard Fmoc strategy.[1] Fmoc-Arg(Pbf)-OH (1.2 eq) was attached to the TCP resin with DIEA (2.5 eq) in anhydrous DCM (2 mL) at room temperature for 1 h. After filtration, the remaining trityl chloride groups were capped by a solution of DCM, MeOH, DIEA (17 : 2 : 1; v : v : v) for 15 min. The resin was filtered and washed thoroughly with DCM (2×), DMF (3×) and MeOH (5×). The loading capacity was determined by weight after drying the resin under vacuum, and ranged from 0.40 to 0.65 mmol/g.

Solid phase Fmoc deprotection

The resin-bound Fmoc peptide was treated with 20% piperidine in NMP (v/v) for 5 min and a second time for 15 min. The resin was washed with NMP (5×)

Solid phase peptide coupling with HOBt / TBTU

A solution of Fmoc-Xaa-OH (3 eq), TBTU (3 eq), HOBt (3 eq), DIEA (6 eq) in NMP was added to the resin-bound free amine peptide and shaken for 1 h at room temperature. The resin was washed with NMP (5×).

Cleavage of side-chain-protected peptides from TCP resin

The resin-bound peptide was treated three times with a 20% solution of HFIP (hexafluoroisopropanol) in DCM (v/v) for 30 min. The collected solutions were concentrated *in vacuo*.

Cleavage and full deprotection of peptides from TCP resin

The resin-bound peptide was treated three times with a mixture of TFA, water, triisopropylsilane (95% : 2.5% : 2.5%, v : v : v) for 1 h. The deprotected peptide precipitated was spun down in a centrifuge after adding diethyl ether, washed twice with ether and dried under vacuum. The deprotection was followed by ESI-MS.

Backbone cyclization of peptides

The head-to-tail cyclization was performed with diphenylphosphorylacid azide (DPPA), applying the solid base method using $NaHCO_3$ in N,N-dimethylformamide (DMF). After the completion of cyclization, which was monitored by ESI mass spectroscopy, DMF was evaporated and the peptide was dissolved in ethyl acetate, which precipitated the cyclization reagents and left the crude product dissolved in ethyl acetate and washed three times with a solution of $NaHCO_3$ and once with brine.

Full deprotection of cyclic peptides

The cyclic peptide was treated with a mixture of TFA, water, triisopropylsilane (95% : 2.5% : 2.5%, v : v : v) for 1 h. The deprotected peptide precipitated was spun down in a centrifuge after adding diethyl ether, washed twice with ether and dried under vacuum. The deprotection was followed by ESI-MS.
The pure compound was obtained by reversed phase high-performance liquid chromatography (RP-HPLC) purification. The peptides were characterized by ESI mass spectroscopy.

4. Characterization of peptides

Compound No.	Sequence	ESI-MS $(M+H)^+$	HPLC-Gradient	Retention time [min]
I	f-*iso*DGR-V	575	10-100%	11.10
II	F-*iso*dGR-V	575	10-100%	11.26
III	F*iso*DGR-V	575	10-100%	11.27
IV	F-*iso*DGr-V	575	10-100%	11.22
V	F-*iso*DGR-v	575	10-100%	11.55
VI	G-isodGR-G	443	0-100%	7.10
VII	G-isoDGr-G	443	0-100%	7.17
VIII	F-isodGR-G	533	10-100%	8.67
IX	F-isoDGr-G	533	10-100%	8.74
X	Hphe-isodGR-G	547	10-100%	10.15
XI	Hphe-isoDGr-G	547	10-100%	10.29
XII	Phg-isodGR-G	519	10-100%	7.18
XIII	Phg-isoDGr-G	519	10-100%	7.06
1	G-isoDGR-G	443	0-100%	7.01
2	F-isoDGR-G	533	10-100%	8.59
3	f-isoDGR-G	533	10-100%	8.02
4	G-isoDGR-F	533	10-100%	8.20
5	G-isodGR-f	533	10-100%	8.02
6	Hphe-isoDGR-G	547	10-100%	9.83
7	hphe-isoDGR-G	547	10-100%	9.54
8	G-isoDGR-Hphe	547	10-100%	9.38
9	G-isoDGR-hphe	547	10-100%	9.53
10	Phg-isoDGR-G	519	10-100%	6.83
11	phg-isoDGR-G	519	10-100%	7.18
12	G-isoDGR-Phg	519	10-100%	7.12
13	G-isoDGr-phg	519	10-100%	7.00

5. Integrin activity data

Compound No.	Sequence	IC50 α5β1 [nM]	IC50 αvβ3 [nM]
I	f-*iso*DGR-V	846	50
II	F-*iso*dGR-V	2004	100
III	F*iso*DGR-V	31892	>1000
IV	F-*iso*DGr-V	>40000	>1000
V	F-*iso*DGR-v	1860	50
VI	G-isodGR-G	7638	>1000
VII	G-isoDGr-G	8035	>1000
VIII	F-isodGR-G	>1700	>1000
IX	F-isoDGr-G	1279	>1000
X	Hphe-isodGR-G	>20000	>1000
XI	Hphe-isoDGr-G	812	>1000
XII	Phg-isodGR-G	7031	>1000
XIII	Phg-isoDGr-G	711	>1000

6. Solid phase binding assay

The inhibiting activity and integrin selectivity of the integrin inhibitors were determined in a solid phase binding assay using soluble integrins and coated extracellular matrix proteins. Binding of integrins was than detected by specific antibodies in an enzyme-linked immunosorbent assay. Fibronectin and vitronectin were purchased from Sigma (St. Louis, MO), the integrin α5β1 was purchased from R&D Systems (Minneapolis, MN) and αVβ3 from Chemicon (Chemicon Europe, Germany). The integrin antibodies were purchased from Pharmingen, BD Bioscience Europe (mouse anti-human CD51/CD61, and mouse anti-human CD49e) and Sigma (anti-mouse-HRP conjugate). The detection of HRP was performed using HRP substrate solution 3.3.5.5'-tetramethylethylenediamine (TMB, Seramun, Germany) and 2 M H_2SO_4 for stopping the reaction. The developed color was measured at 450 nm with a POLARstar Galaxy plate reader (BMG Labtechnologies). Every concentration was analyzed by duplicate and the resulting inhibition curves were analyzed using OriginPro 7.5G software, the turning point describes the IC_{50} value.

α5β1: BRAND flat-bottom 96-well ELISA plates were coated over night at 4°C with fibronectin (0.50 µg/mL) in 15 mM Na_2CO_3, 35 mM $NaHCO_3$, pH 9.6. Plates were subsequently washed three times with PBST buffer (137 mM NaCl, 2.7 mM KCl, 10 mM Na_2HPO_4, 2 mM KH_2PO_4, 0.01% Tween 20, pH 7.4) and blocked for one hour at room temperature with 150 µL/well of TSB-buffer (20 mM Tris-HCl, 150 mM NaCl, 1 mM $CaCl_2$, 1 mM $MgCl_2$, 1 mM $MnCl_2$, pH 7.5, 1% BSA). Soluble integrin α5β1 (1.0 µg/mL) and a serial dilution of integrin inhibitor in TSB were incubated in the coated wells for 1 h at room temperature. The plate was then washed three times with PBST buffer and 100 µL/well of primary antibody (CD49e) were incubated at 1.0 µg/mL in TSB (1:500 dilution) for 1 h at room temperature. After washing tree times with PBST, 100 µL/well of the secondary anti-body (anti-mouse-HRP conjugate) were applied at 2.0 µg/mL in TSB (1:385 dilution) for 1 h at room temperature. After this treatment the plate was washed three times and the binding visualized as described above.

For the αvβ3 assay, plates were coated with vitronectin (1.0 µg/mL) and blocked as described for α5β1. Soluble αVβ3 (1.0 µg/mL) was incubated with a serial dilution of integrin inhibitor for one hour at room temperature. Primary (CD51/CD61, 2.0 µg/mL, 1:250 dilution) and secondary antibody (anti-mouse-HRP conjugate, 1.0 µg/mL, 1:770 dilution) were applied each for 1 h at room temperature and the binding visualized as described above.

The peptides **I** to **XIII** were tested by Jerini AG with a slightly different method.[2]

7. NMR Spectroscopy of the peptides 11 and 13

Each 5 mg of the peptides **11** and **13** were dissolved in 500 µl d_6-DMSO; the solvent was also used for the lock signal. All spectra were recorded on a Bruker DMX500 spectrometer equipped with a 5 mm TXI RT probe head and referenced to the B_0 magnetic field. Purity and conformational equilibria of the compounds were checked via ^{1}H-1D spectra. For both peptides, only one signal set was observed in the NMR spectra. Atom and atom group assignment was done via E.COSY[3] and TOCSY[4] spectra; sequential assignment was accomplished by through-bond connectivities from heteronuclear multiple bond correlation (^{1}H,^{13}C-HMBC)[5] spectra. Connectivities were proved by interresidual scalar couplings, e.g between carbonyl carbons and adjacent amide protons. ROESY[6] spectra were recorded to extract information about pair-wise proton-proton distances. Homonuclear J-couplings were extracted from E.COSY spectra. For TOCSY, ROESY, and E.COSY spectra, 16 k data points were recorded in the direct dimensions and 512 data points in the indirect dimensions (2 k data points for E.COSY). QSINE window functions and zero filling to twice the number of recorded points were used for processing. HMBC spectra were recorded with 4 k data points in the F2 and 256 data points in the F1 dimensions; for processing, SINE and QSINE functions as well as zero filling to twice the number of recorded points were used. TOCSY spectra were recorded with a mixing time of 80 ms, ROESY spectra with a mixing time of 150 ms, thus avoiding unwanted effects caused by spin diffusion. The temperature of all measurements was 300 K. The software tools TOPSPIN and SPARKY were utilized to process spectra, to assign resonances, and for ROE peak volume integration. Proton distances were calculated according to the isolated two-spin approximation.[7] No ROE offset correction was performed since biasing offset effects at the field strength used in this study are rather small. The integrated volumes of ROE cross peaks were converted to proton–proton distances by the help of calibration to distances between methylene protons (1.78 Å). Upper and lower distance restraints were obtained by adding and subtracting 10 % to / from the calculated experimental values, thus accounting for experimental errors and simulation uncertainties.

8. Structure calculation of the peptides 11 and 13

Calculation of the most representative conformations of **11** and **13** was done by distance geometry (DG) and molecular dynamics (MD) simulations. Metric matrix DG calculations were carried out with a distance geometry algorithm utilizing random metrization.[8] Experimental distance restraints which are more restrictive than the geometric distance bounds (holonomic restraints) were used to create the final distance matrix. All structure templates were first embedded in four dimensions and then partially minimized using conjugate gradient minimization followed by distance-driven dynamics (DDD) wherein only distance constraints were used.[9] The DDD simulation was carried out at 1000 K for 50 ps with a gradual reduction in temperature over the next 30 ps. The DDD procedure utilized holonomic and experimental distance constraints plus a chiral penalty function for the generation of violation energies and forces. A distance matrix was calculated from each structure, and the EMBED algorithm was used to compute Cartesian coordinates in three dimensions.[10] 50 structures were calculated for each peptide, and > 95 % of the structure bundles of both peptides did not show any significant violations (> 0.12 Å). MD calculations were carried out with the program Gromacs version 3.3.3.[11] The Gromos G53a6 force field as implemented in Gromacs was used for parametrization of the peptide and DMSO solvent molecules.[12] The most representative DG structures of the peptides were first energy minimized by the conjugate-gradient[13] algorithm and then placed in truncated octahedral simulation boxes with the box walls being at least 1.6 nm away from the solutes. The boxes were each filled with more than 600 DMSO solvent molecules and subsequently energy minimized with the steepest descent algorithm whereas all atoms of the solutes were positionally restrained to their original positions (F = 2.5 E+005 kJ / mol). Afterwards, both boxes were heated up to 360 K (higher simulation temperatures compared to experimental ones in order to overcome higher energy barriers) in six steps and the position restraints were stepwise lowered until the positional forces reach 0 kJ / mol (each equilibrium run was simulated for 50 ps). The average temperature was maintained via the Berendsen[14] algorithm as implemented in Gromacs 3.3.3. Then, Berendsen pressure coupling[14] was turned on for 500 ps. Production runs were 250 ns long. Intermolecular interactions were treated with a twin-range cutoff of 0.8 nm and 1.4 nm. The pair-lists were updated each after five integration steps. Behind the long-range cutoff, a reaction-field (epsilon_rf = 38) was used to calculate long-range Coulombic interactions. A leap-frog algorithm was utilized to integrate Newton's equation of motion with a integration time step of 2 fs.[15] All bonds were constrained applying the SHAKE[16] algorithm. In addition, periodic boundary conditions were utilized and the center-of-mass motion was removed every 500 integration steps. The two peptides were simulated both as fully neutral (ARG and isoASP uncharged) and as zwitter ionic (ARG and isoASP charged) species in separated runs. Evaluation of ROE based distance restraints and of J-couplings was performed via tools as implemented in the Gromos2005 MD software package.[17] Pseudo-atom and multiplicity corrections for distance restraints were applied as described by Koning et al.[18] The peptides were presented in Fig. 2 as vacuum energy minimized conformations.

9. NMR & MD data for peptide 11: c(-DPhg-lasp-Gly-Arg-Gly-)

a) Assignment (given in ppm)

1DPHG			2IASP			3GLY			4ARG			5GLY		
NH	---	8.60	**NH**	---	7.84	**NH**	---	8.42	**NH**	---	8.42	**NH**	---	8.03
HA	---	5.50	**HA**	---	4.47	**HA1**	pro-R	3.61	**HA**	---	4.06	**HA1**	pro-R	3.70
HD*	---	7.46	**HB1**	pro-R	2.57	**HA2**	pro-S	3.89	**HB1**	pro-R	1.61	**HA2**	pro-S	3.88
HE*	---	7.35	**HB2**	pro-S	2.82				**HB2**	pro-S	1.79			
HZ	---	7.33							**HG***	---	1.51			
									HD*	---	3.12			
									HE	---	7.66			

b) ROE distance restraints

Assignment					Experimental (Å)		Zwitter (Å)		Uncharged (Å)		Combined (Å)	
No	**AS-1**	**At-1**	**AS-2**	**At-2**	**Upper**	**Lower**	**Calc**	**Viol**	**Calc**	**Viol**	**Calc**	**Viol**
01	1DPHG	NH	1DPHG	HA	**3.20**	**2.62**	**2.68**		**2.72**		**2.70**	
02	2IASP	NH	1DPHG	HA	**3.54**	**2.90**	**3.13**		**2.87**	**- 0.03**	**3.00**	
03	2IASP	NH	2IASP	HA	**2.84**	**2.32**	**2.69**		**2.73**		**2.71**	
04	3GLY	NH	2IASP	HA	**4.21**	**3.45**	**4.02**		**3.81**		**3.92**	
05	2IASP	NH	2IASP	HB1	**3.75**	**3.07**	**3.35**		**3.18**		**3.27**	
06	3GLY	NH	2IASP	HB1	**3.00**	**2.46**	**2.60**		**3.35**	**+ 0.35**	**2.85**	
07	2IASP	NH	2IASP	HB2	**3.56**	**2.92**	**2.63**	**- 0.29**	**3.78**	**+ 0.22**	**2.97**	
08	3GLY	NH	2IASP	HB2	**2.64**	**2.16**	**2.39**		**2.28**		**2.33**	
09	1DPHG	NH	2IASP	NH	**2.77**	**2.27**	**2.49**		**2.64**		**2.55**	
10	4ARG	NH	4ARG	HA	**3.14**	**2.56**	**2.76**		**2.13**	**- 0.43**	**2.39**	**- 0.17**
11	5GLY	NH	4ARG	HA	**2.76**	**2.26**	**2.82**	**+ 0.06**	**2.19**	**- 0.07**	**2.46**	
12	4ARG	HA	4ARG	HB2	**2.87**	**2.35**	**2.57**		**2.49**		**2.54**	
13	4ARG	HE	4ARG	HB2	**3.71**	**3.03**	**3.48**		**3.78**	**+ 0.07**	**3.60**	
14	4ARG	NH	4ARG	HB2	**3.37**	**2.75**	**3.11**		**3.66**	**+ 0.29**	**3.32**	
15	1DPHG	NH	5GLY	HA2	**3.01**	**2.47**	**2.34**	**- 0.13**	**2.41**	**- 0.06**	**2.37**	**- 0.10**
16	1DPHG	NH	5GLY	HA1	**3.35**	**2.75**	**3.18**		**3.29**		**3.23**	
17	1DPHG	NH	5GLY	NH	**3.09**	**2.53**	**3.17**	**+ 0.08**	**2.83**		**3.00**	
18	4ARG	NH	5GLY	NH	**3.16**	**2.58**	**2.60**		**3.07**		**2.78**	
19	2IASP	HA	2IASP	HB1	**2.68**	**2.20**	**2.40**		**2.34**		**2.37**	
20	3GLY	NH	2IASP	NH	**3.69**	**3.01**	**3.90**	**+ 0.21**	**3.82**	**+ 0.13**	**3.86**	**+ 0.17**
21	5GLY	NH	2IASP	NH	**3.95**	**3.23**	**3.99**	**+ 0.04**	**2.86**	**- 0.37**	**3.29**	
22	5GLY	NH	5GLY	HA1	**2.93**	**2.39**	**2.65**		**2.73**		**2.69**	
23	5GLY	NH	5GLY	HA2	**2.93**	**2.39**	**2.57**		**2.50**		**2.54**	
24	1DPHG	NH	4ARG	NH	**5.39**	**4.41**	**5.16**		**5.18**		**5.17**	
25	3GLY	NH	3GLY	HA1	**2.73**	**2.23**	**2.29**		**2.28**		**2.28**	
26	3GLY	NH	3GLY	HA2	**2.52**	**2.06**	**2.66**	**+ 0.14**	**2.73**	**+ 0.21**	**2.69**	**+ 0.17**
27	2IASP	HA	2IASP	HB2	**2.95**	**2.41**	**2.70**		**2.34**	**- 0.07**	**2.51**	

Assignment					Experimental (Å)		Zwitter (Å)		Uncharged (Å)		Combined (Å)	
28	1DPHG	HE*	1DPHG	HA	5.74	2.98	4.71		4.71		4.71	
29	1DPHG	NH	1DPHG	HE*	6.22	3.38	4.96		4.80		4.88	
30	2IASP	NH	1DPHG	HE*	6.80	3.84	5.37		6.03		5.63	
31	1DPHG	NH	1DPHG	HD*	5.30	2.62	2.70		2.61	- 0.01	2.66	
32	2IASP	NH	1DPHG	HD*	5.95	3.15	3.19		3.57		3.35	
33	4ARG	HD*	4ARG	HB2	4.00	2.54	2.83		2.93		2.87	
34	4ARG	HA	4ARG	HD*	4.20	2.70	3.64		3.11		3.35	

c) J-Couplings

Assignment				Zwitter (Hz)			Uncharged (Hz)			Combined (Hz)		
AS	At-1	At-2	Chiral	Exp	Calc	Viol	Exp	Calc	Viol	Exp	Calc	Viol
1DPHG	NH	HA	---	8.5	8.0	0.5	8.5	8.0	0.5	8.5	8.0	0.5
2IASP	NH	HA	---	7.9	7.5	0.4	7.9	6.9	1.0	7.9	7.3	0.6
2IASP	HA	HB1	pro-R	4.1	3.3	0.8	4.1	3.2	0.9	4.1	3.3	0.8
2IASP	HA	HB2	pro-S	7.0	9.4	2.4	7.0	3.8	3.2	7.0	6.9	0.1
3GLY	NH	HA1	pro-R	5.4	5.3	0.1	5.4	6.0	0.6	5.4	5.7	0.3
3GLY	NH	HA2	pro-S	6.6	5.8	0.8	6.6	5.5	1.1	6.6	5.7	0.9
4ARG	NH	HA	---	6.2	8.0	1.8	6.2	6.7	0.5	6.2	7.4	1.2
4ARG	HA	HB1	pro-R	9.0	8.7	0.3	9.0	11.1	2.1	9.0	9.8	0.8
4ARG	HA	HB2	pro-S	5.6	5.2	0.4	5.6	3.8	1.8	5.6	4.5	1.1
5GLY	NH	HA1	pro-R	5.0	5.4	0.4	5.0	4.2	0.8	5.0	4.9	0.1
5GLY	NH	HA2	pro-S	6.9	5.1	1.8	6.9	7.2	0.3	6.9	6.1	0.8

d) Remarks

DPHG: D-phenylglycine, IASP: iso-aspartic acid

The MD runs of **11** as zwitter ionic and uncharged peptide result in obvious violations of ROE based distance restraints and of scalar couplings. If both runs, each 250 ns long, are combined (the first frame of the "zwitter ionic run" is added to last frame of the "uncharged run") to one trajectory of 500 ns length, and pairwise proton distances and dihedral angle averages are evaluated again, all parameters are in very good agreement with the experimentally yielded NMR data. The table below shows the population of clustered peptide family members of **11** arising within the 500 ns trajectory (based on a backbone RMSD cut-off of 0.4 Å using the Gromos cluster[19] algorithm). Remaining violations show that the available conformational space of **11** was not completely sampled. For our computational docking runs, the two most representative conformations ("Structure 1 & 2") of **11** were used but only the uncharged species led to meaningful results as presented in the main text. Hence, only this conformation was discussed in the manuscript.

Structure 1	Structure 2	Structure 3	Structures 4-26
48 % (Zwitter)	32 % (Uncharged)	7 %	13 %

10. NMR & MD data for peptide 13: c(-DPhg-Gly-lAsp-Gly-Arg-)

a) Assignment (given in ppm)

1DPHG			2GLY			3lASP			4GLY			5ARG		
NH	---	8.61	**NH**	---	8.65	**NH**	---	7.77	**NH**	---	8.47	**NH**	---	8.02
HA	---	5.27	**HA1**	pro-R	3.66	**HA**	---	4.48	**HA1**	pro-R	3.56	**HA**	---	4.32
HD*	---	7.39	**HA2**	pro-S	3.78	**HB1**	pro-R	2.63	**HA2**	pro-S	3.79	**HB1**	pro-R	1.51
HE*	---	7.35				**HB2**	pro-S	2.78				**HB2**	pro-S	1.73
HZ	---	7.37										**HG***	---	1.41
												HD*	---	3.09
												HE	---	7.57

b) ROE distance restraints

Assignment					Experimental (Å)		Zwitter (Å)		Uncharged (Å)		Combined (Å)	
No	**AS-1**	**At-1**	**AS-2**	**At-2**	**Upper**	**Lower**	**Calc**	**Viol**	**Calc**	**Viol**	**Calc**	**Viol**
01	1DPHG	HA	1DPHG	NH	**3.45**	**2.82**	**2.77**	**- 0.05**	**2.80**	**- 0.02**	**2.79**	**- 0.03**
02	1DPHG	HA	2GLY	NH	**2.81**	**2.30**	**2.39**		**2.37**		**2.38**	
03	2GLY	NH	2GLY	HA2	**3.06**	**2.50**	**2.63**		**2.67**		**2.65**	
04	2GLY	NH	2GLY	HA1	**3.07**	**2.51**	**2.46**	**- 0.05**	**2.39**	**- 0.12**	**2.43**	**- 0.08**
05	3lASP	NH	2GLY	HA1	**3.43**	**2.81**	**3.19**		**3.23**		**3.21**	
06	2GLY	NH	3lASP	NH	**3.24**	**2.65**	**3.65**	**+ 0.42**	**3.05**		**3.30**	**+ 0.07**
07	3lASP	NH	3lASP	HA	**2.97**	**2.43**	**2.76**		**2.72**		**2.74**	
08	4GLY	NH	3lASP	HA	**4.06**	**3.32**	**3.59**		**3.64**		**3.62**	
09	3lASP	NH	3lASP	HB1	**4.38**	**3.58**	**3.51**	**- 0.07**	**3.34**	**- 0.24**	**3.42**	**- 0.16**
10	4GLY	NH	3lASP	HB1	**3.20**	**2.62**	**2.84**		**3.42**	**+ 0.22**	**3.08**	
11	3lASP	NH	3lASP	HB2	**3.86**	**3.16**	**2.49**	**- 0.67**	**3.81**		**2.89**	**- 0.27**
12	4GLY	NH	3lASP	HB2	**2.90**	**2.38**	**2.33**	**- 0.05**	**2.52**		**2.41**	
13	5ARG	NH	4GLY	HA2	**3.54**	**2.90**	**3.07**		**3.16**		**3.11**	
14	5ARG	NH	4GLY	HA1	**3.15**	**2.58**	**2.25**	**- 0.33**	**2.46**	**- 0.12**	**2.35**	**- 0.23**
15	1DPHG	NH	5ARG	NH	**3.80**	**3.11**	**3.98**	**+ 0.17**	**3.52**		**3.72**	
16	4GLY	NH	5ARG	NH	**3.56**	**2.91**	**4.06**	**+ 0.51**	**2.98**		**3.36**	
17	1DPHG	NH	5ARG	HA	**2.61**	**2.14**	**2.19**		**2.17**		**2.18**	
18	5ARG	NH	5ARG	HA	**3.38**	**2.76**	**2.74**	**- 0.02**	**2.46**	**- 0.30**	**2.58**	**- 0.18**
19	5ARG	NH	5ARG	HB2	**3.16**	**2.59**	**2.41**	**- 0.18**	**2.65**		**2.52**	**- 0.07**
20	5ARG	HA	5ARG	HB2	**2.95**	**2.41**	**2.70**		**2.74**		**2.72**	
21	5ARG	HE	5ARG	HB2	**3.64**	**2.98**	**3.55**		**3.66**	**+ 0.02**	**3.61**	
22	5ARG	NH	5ARG	HB1	**3.81**	**3.12**	**3.07**	**- 0.05**	**3.33**		**3.19**	
23	5ARG	HA	5ARG	HB1	**3.09**	**2.53**	**2.57**		**2.52**	**- 0.01**	**2.55**	
24	1DPHG	NH	1DPHG	HD*	**4.23**	**2.72**	**2.66**	**- 0.06**	**2.78**		**2.72**	
25	1DPHG	HD*	2GLY	NH	**5.16**	**3.48**	**3.56**		**3.46**	**- 0.02**	**3.51**	
26	5ARG	HD*	5ARG	HB2	**3.62**	**2.22**	**2.87**		**2.99**		**2.93**	
27	5ARG	HD*	5ARG	HB1	**4.19**	**2.69**	**2.84**		**2.85**		**2.85**	

Assignment					Experimental (Å)		Zwitter (Å)		Uncharged (Å)		Combined (Å)	
28	5ARG	HA	5ARG	HD*	4.59	3.02	3.57		3.33		3.44	
29	5ARG	HG*	5ARG	NH	4.87	3.24	3.28		3.44		3.36	
30	5ARG	HA	5ARG	HG*	4.30	2.78	2.68	- 0.10	2.74	- 0.04	2.71	- 0.07
31	5ARG	HB1	5ARG	HG*	3.88	2.44	2.47		2.47		2.47	
32	1DPHG	NH	1DPHG	HE*	5.36	3.65	4.89		5.09		4.99	
33	1DPHG	HA	1DPHG	HE*	4.81	3.20	4.70		4.69		4.69	

c) J-Couplings

Assignment				Zwitter (Hz)			Uncharged (Hz)			Combined (Hz)		
AS	At-1	At-2	Chiral	Exp	Calc	Viol	Exp	Calc	Viol	Exp	Calc	Viol
1DPHG	NH	HA	---	7.3	8.6	1.3	7.3	7.7	0.4	7.3	8.1	0.8
2GLY	NH	HA1	pro-R	6.4	6.7	0.3	6.4	5.7	0.7	6.4	6.2	0.2
2GLY	NH	HA2	pro-S	5.9	5.5	0.4	5.9	5.9	0.0	5.9	5.7	0.2
3IASP	NH	HA	---	8.2	7.0	1.2	8.2	8.2	0.0	8.2	7.6	0.6
3IASP	HA	HB1	pro-R	3.5	3.6	0.1	3.5	2.8	0.7	3.5	3.2	0.3
3IASP	HA	HB2	pro-S	7.5	3.5	4.0	7.5	11.2	3.7	7.5	7.4	0.1
4GLY	NH	HA1	pro-R	5.4	5.7	0.3	5.4	4.7	0.7	5.4	5.2	0.2
4GLY	NH	HA2	pro-S	6.5	6.4	0.1	6.5	7.0	0.5	6.5	6.7	0.2
5ARG	NH	HA	---	7.3	7.3	0.0	7.3	6.7	0.6	7.3	7.0	0.3
5ARG	HA	HB1	pro-R	8.5	9.8	1.3	8.5	8.7	0.2	8.5	9.2	0.7
5ARG	HA	HB2	pro-S	5.4	4.7	0.7	5.4	5.5	0.1	5.4	5.1	0.3

d) Remarks

DPHG: D-phenylglycine, IASP: iso-aspartic acid

The MD runs of **13** as zwitter ionic and uncharged peptide result in obvious violations of ROE based distance restraints and of scalar couplings. If both runs, each 250 ns long, are combined (the first frame of the "zwitter ionic run" is added to last frame of the "uncharged run") to one trajectory of 500 ns length, and pairwise proton distances and dihedral angle averages are evaluated again, all parameters are in excellent agreement with the experimentally yielded NMR data. The table below shows the population of clustered peptide family members of **13** arising within the 500 ns trajectory (based on a backbone RMSD cut-off of 0.4 Å using the Gromos cluster[19] algorithm). Remaining violations show that the available conformational space of **13** was not completely sampled. For our computational docking runs, only the most representative conformation ("Structure 1") of **13** was used, and only this conformation (uncharged) was discussed throughout our manuscript.

Structure 1	Structure 2	Structure 3	Structures 4-20
62 % (Uncharged)	18 % (Zwitter)	9 %	11 %

Conformational Details of Peptide 11 (as shown in the main text in Fig. 2)

Residue	Torsion	Value	Residue	Torsion	Value
1DPHG	Phi	103°	4ARG	Phi	-85°
	Psi	36°		Psi	-47°
2IASP	Pseudo-Phi	164°	5GLY	Phi	-176°
	Pseudo-Psi	-66°		Psi	97°
	Iso-Bond	170°			
3GLY	Phi	90°			
	Psi	-102°			

Distance 2IASP-CA - 4ARG-CA	Distance 2IASP-CG - 4ARG-CB	Plane Twist Angle 2IASP-CG-CA - 4ARG-CA-CB
7.0 Å	9.4Å	161°

Conformational Details of Peptide 13 (as shown in the main text in Fig. 2)

Residue	Torsion	Value	Residue	Torsion	Value
1DPHG	Phi	86°	4GLY	Phi	83°
	Psi	-117°		Psi	-126°
2GLY	Phi	-119°	5ARG	Phi	-86°
	Psi	118°		Psi	124°
3IASP	Pseudo-Phi	124°			
	Pseudo-Psi	-60°			
	Iso-Bond	149°			

Distance 2IASP-CA - 4ARG-CA	Distance 2IASP-CG - 4ARG-CB	Plane Twist Angle 2IASP-CG-CA - 4ARG-CA-CB
7.1 Å	9.9 Å	164°

11. Molecular docking

Methods

Docking simulations

Molecular docking of **11** and **13** in the X-ray three-dimensional structure of αvβ3 (PDB code: 1L5G) and in the α5β1 homology model published before, was carried out using the AutoDock 4.0 software package as implemented through the graphical user interface AutoDockTools (ADT 1.5.2).[20]

Ligands and protein setup

The conformations of peptides **11** and **13** as experimentally determined by NMR, distance geometry, and subsequent molecular dynamics (restrained MD) were used as docking starting structures (after energy minimization in vacuum). During the docking process the backbone conformation was held fix, while the side chain dihedral angles were free to rotate. Partial atomic charges were assigned by using the Gasteiger-Marsili formalism.

Docking setup

The docking area has been defined by a box, centered on the coordinate of the metal in the MIDAS region. Grid points of 70×70×70 with 0.375 Å spacing were calculated around the docking area for all the ligand atom types using AutoGrid4. For each ligand, 100 separate docking calculations were performed. Each docking calculation consisted of 10 million energy evaluations using the Lamarckian genetic algorithm local search (GALS) method. A low-frequency local search according to the method of Solis and Wets was applied to docking trials to ensure that the final solution represents a local minimum. Each docking run was performed with a population size of 150, and 300 rounds of Solis and Wets local search were applied with a probability of 0.06. A mutation rate of 0.02 and a crossover rate of 0.8 were used to generate new docking trials for subsequent generations. The GALS method evaluates a population of possible docking solutions and propagates the most successful individuals from each generation into the next one. The docking results from each of the 100 calculations were clustered on the basis of root-mean square deviation (rmsd = 1.5 Å) between the Cartesian coordinates of the ligand atoms and were ranked on the basis of the free energy of binding. However, for each ligand, the free energy of binding as well as the consonance with experimental data, such as receptor-mutagenesis and ligands SARs, were taken into account for the choice of the published binding modes.

Further details on the docking of 11 into the αvβ3, implication for ligand selectivity and comparison with Cilengitide

Predictably, the described favorable binding pose of **11** in αvβ3 cannot be found in the same receptor due to the fact that the pocket below the SDL is remarkably narrower in αvβ3 with respect to α5β1 due to the substitution of (β1)-Leu219, (β1)-Ser171, (β1)-Gly217 with (β3)-Arg216 (β3)-Tyr166 (β3)-Arg214 respectively. Indeed, in the search of α5β1- selective ligands we were

previously successful in targeting this region.[21] Moreover, docking calculations of **11** into the avb3 receptor suggest a certain difficulty for the Arg guanidinium group to insert into the narrow groove at the top of the propeller domain, where salt bridge to Asp218 and/or Asp150 should occur. In fact over 100 proposed conformation, only10 display one of the two salt bridges (one of the ten is shown in Figure SI_2 superimposed to the experimental binding mode of Cilengitide). Probably, this is due to the peculiar conformation of the peptidic cycle together with the forced position of the phenyl ring which cannot occupy the wide pocket below the SDL peculiar of the $\alpha 5\beta 1$ receptor. This evidence together with the unfavourable position of the phg phenyl ring seems to be the reason for a low binding to the $\alpha v\beta 3$ receptor.

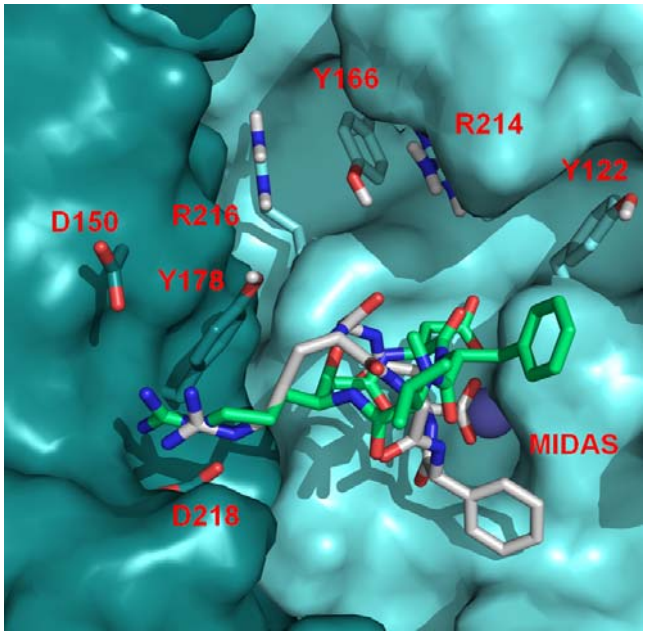

Figure SI_2: Superposition of a theoretical binding mode of **11** (white) and the experimental (X-ray) binding mode of Cilengetide (green) in $\alpha v\beta 3$.

Further details on docking calculations of 13 in a5b1, implication for ligand selectivity and comparison with Cilengitide

Docking studies of **13** in α5β1 receptor resulted in an ambiguous position of the phg aromatic ring within the RGD binding pocket. Indeed, two main poses were found, which have in common the interactions with metal in the MIDAS and with D227 side chain and which primarily differ for the orientation of the phg aromatic ring (see Figure SI_3). Interestingly, the two binding modes show similar free energy of binding and this is in perfect line with the observation that in both orientation the phg aromatic ring of **13** does not engage any strong interaction with the receptor residues as found when docking of **13** was performed in αvβ3. Thus, it seems that the favourable interactions between the phg aromatic ring of **13** and the (αv)-Tyr178, (β3)-Tyr166, (β3)-Arg214 residues, which are characteristic for αvβ3, are the reason for an higher binding to the αvβ3 receptor.

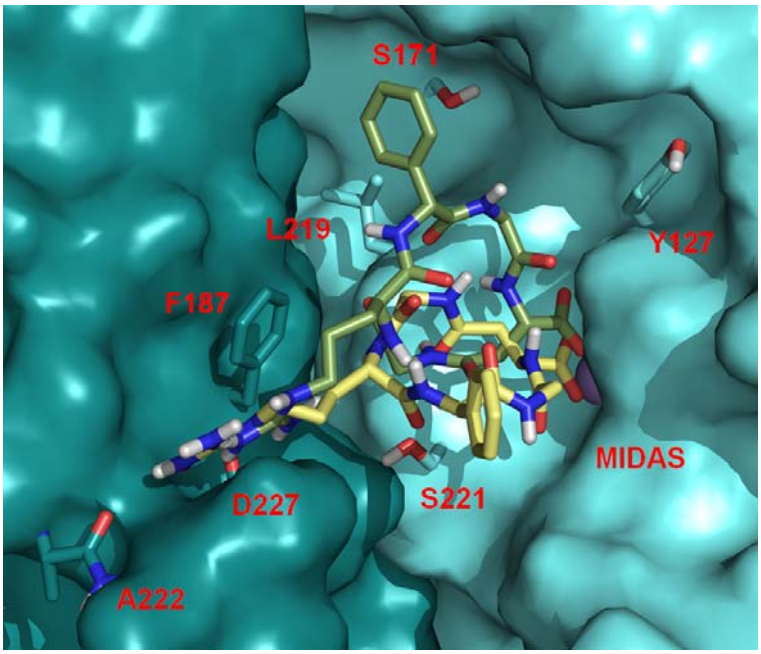

Figure SI_3: The two main binding poses of **13** (yellow and green) in the α5β1 integrin binding pocket.

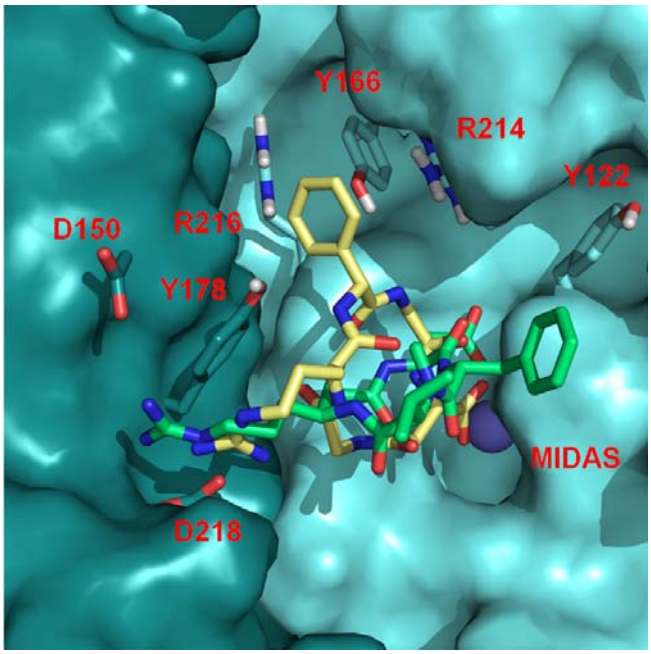

Figure SI_4: Superposition of theoretical binding mode of **13** (yellow) and experimental (X-ray) binding mode of Cilengetide (green) in αvb3. Although the aromatic ring in 13 and Cilengitide are differently oriented, both are able to establish favorable contacts with the receptor residues (see main text of the manuscript for the description of interactions).

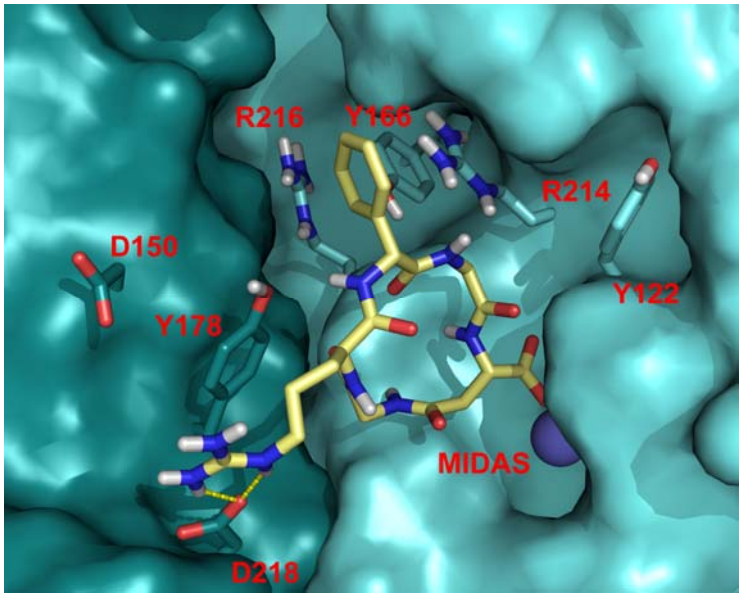

Figure SI_5: Docked structure (alternative pose) of **13** (pale yellow) in the αvβ3 integrin binding pocket. The αv and β3 subunits are represented by the blue and cyan surface respectively. In both subunits amino acid side chains important for the ligand binding are highlighted as sticks. The metal ion in the MIDAS region is represented by a purple sphere.

Ability of Cilengetide to fit the a5b1 binding pocket

The ability of Cilengitide to bind the RGD binding site of the a5b1 homology model was tested in 2005 for a previous work focused on the a5b1 receptor (J. Med. Chem. 2005, 48, 4166 – 4204.). It was found that Cilengitide binds the a5b1 in the same manner as found experimentally for avb3. However, the attachment of the Arg guanidinium moiety of the Cilengitide to the a5b1 propeller domain is expected to be less strong with respect to that to $\alpha v\beta 3$ due to the substitution of αv-D150 with α5-A159.

12. Cell assays

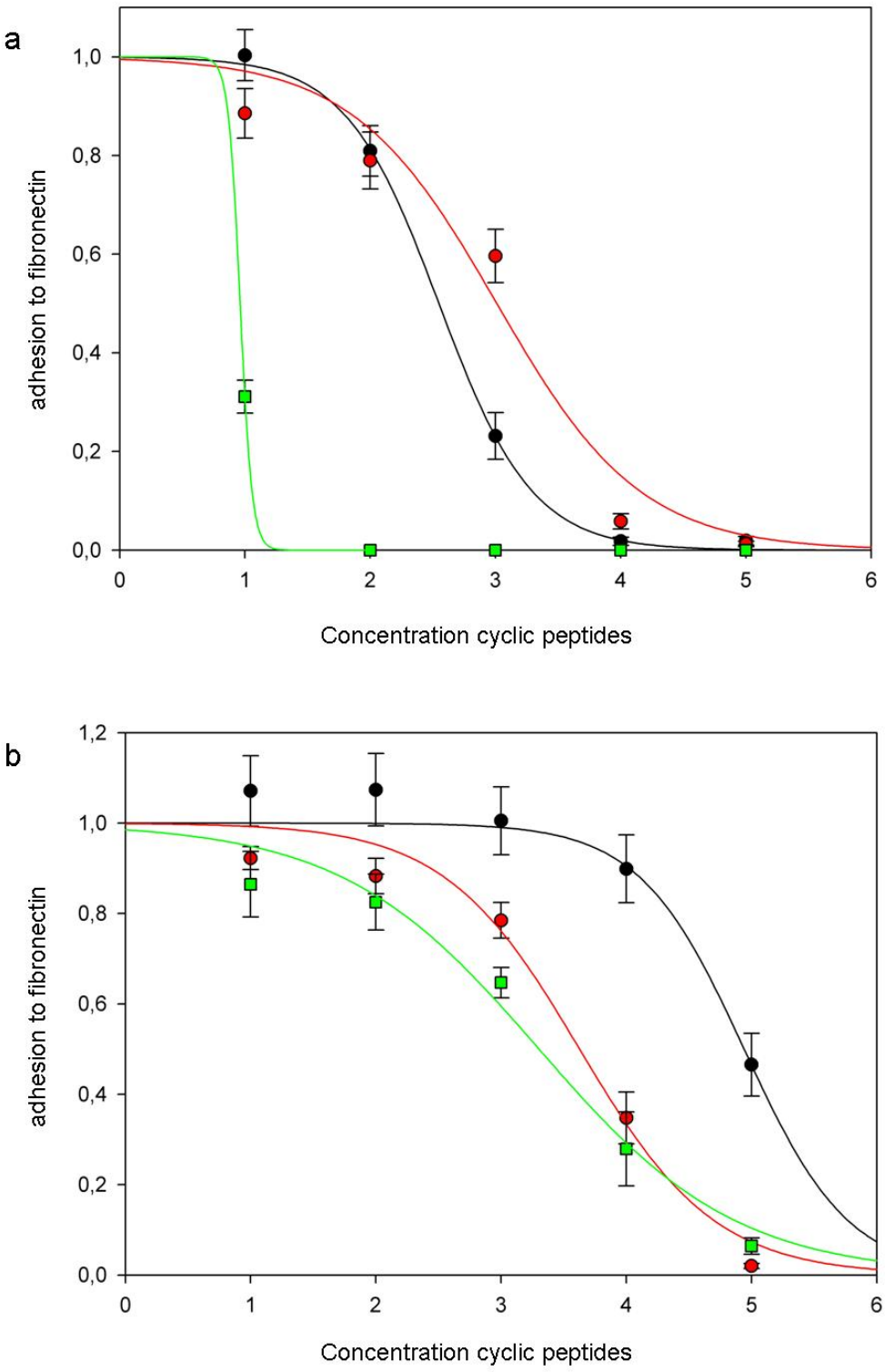

Figure SI_6: a) Blocking assay of Cilengitide (green), **11** (rot) and **13** (black) with αvβ3 expressing cells. b) Assay with α5β1 expressing cells; 1 = 10 nM, 2 = 100 nM, 3 = 1000 nM, 4 = 10000 nM, 5 = 100000 nM

Cells

Mouse fibroblast cell lines expressing either αvβ3 or α5β1 were generated from fibroblasts derived from the kidney of $\alpha_v^{flox/flox}$, $\beta_1^{flox/flox}$, $\beta_2^{-/-}$, $\beta_7^{-/-}$ mice (manuscript in preparation). Cells were immortalized by retroviral transduction of the SV40 large T and cloned. Subsequently the cells were retrovirally transduced with mouse αv or β1 integrin expression constructs. Endogenous β1 and αv integrin loci were deleted by adenoviral cre-recombinase transduction. Selective expression of αvβ3 or α5β1 was verified by flow cytometry and immunoblotting.

Adhesion blocking assay

To evaluate cell adhesion 96 well plates were coated for 2 h at room temperature with 5µg/mL fibronectin in PBS and then blocked with 1% bovine serum albumin. Fibroblasts expressing αvβ3 or α5β1 were incubated with increasing concentrations (10 - 100000 nM) of the cyclic peptides for 20 min. on ice. Then 40000 cells/well were seeded onto the fibronectin coated plates in presence of the cyclic peptides and incubated for 40 minutes at 37°C. After washing off non-adherent cells the adherent cells were fixed, stained with crystal violet and the relative percentage of adherent cells was determined as previously described.[22] The percentage of adherent cells treated with increasing cyclic peptide concentrations relative to untreated cells was calculated from 3 independent experiments (n=16; means and standard error of the means are shown). To calculate IC_{50} values dose response curves were fitted onto the data using the SigmaPlot software.

Relative binding activities

Comparing the ratios of the respective IC_{50} values shows that in fact the selectivity of peptide **11** is the same for the two independent experimental systems. The selectivity of peptide **13** however was slightly better in the competitive solid phase ELISA. Overall, there is a good correlation between the two observations.

IC_{50} ratios	α5β1 cell line	αvβ3 cell line
Cellular adhesion blocking assay:		
Ratio IC50 11/13	0.05	2.8
Ratio IC50 Cil/11	0.47	0.009
Ratio IC50 Cil/13	0.09	0.02
Competitive solid phase ELISA:		
Ratio IC50 11/13	0.05	11.23
Ratio IC50 cil/11	0.78	0.00054
Ratio IC50 cil/13	0.04	0.006

13. References

[1] G. B. Fields, R. L. Noble, *Int. J. Pept. Protein Res.* **1990**, *35*, 161-214.

[2] D. Heckmann, A. Meyer, L. Marinelli, G. Zahn, R.Stragies, H. Kessler, *Angew. Chem.* **2007**, *119*, 3641-3644; *Angew. Chem. Int. Ed.* **2007**, *46*, 3571-3574.

[3] C. Griesinger, O. W. Sørensen, R. R. Ernst, *J. Magn. Reson*. **1987**, *75*, 474-492.

[4] J. Cavanagh, M. Rance, *J. Magn. Reson.* **1990**, *88*, 72-85.

[5] A. Bax, M. F. Summers, *J. Am. Chem. Soc.* **1986**, *108*, 2093-2094.

[6] C. Griesinger, R. R. Ernst, *J. Magn. Reson.* **1987**, *75*, 261-271.

[7] H. Kessler, C. Griesinger, R. Kerssebaum, K. Wagner, R. R. Ernst, *J. Am. Chem. Soc.* **1987**, *109*, 607-609.

[8] T. F. Havel, *Prog. Biophys. Mol. Biol.* **1991**, *56*, 43-78.

[9] D. F. Mierke, A. Geyer, H. Kessler, *Int. J. Pept. Protein Res.* **1994**, *44*, 325-331.

[10] T. Havel, *Biopolymers* **1990**, *29*, 1565-1585.

[11] H. J. C. Berendsen, D. van der Spoel, R. van Drunen, *Comp. Phys. Comm.* **1995**, *91*, 43-56.

[12] C. Oostenbrink, T. A. Soares, N. F. A. van der Vegt, W. F. van Gunsteren, *Eur. Biophys. J.* **2005**, *34*, 273-284.

[13] K. Zimmerman, *J. Comp. Chem.* **1991**, *12*, 310-319.

[14] H. J. C. Berendsen, J. P. M. Postma, A. DiNola, J. R. Haak, *J. Chem. Phys.* **1984**, *81*, 3684-3690.

[15] R. W. Hockney, S. P. Goel, J. Eastwood, *J. Comp. Phys.* **1974**, *14*, 148-158.

[16] J. P. Ryckaert, G. Ciccotti, H. J. C. Berendsen, *J. Comp. Phys.* **1977**, *23*, 327-341.

[17] M. Christen, P. H. Hünenberger, D. Bakowies, R. Baron, R. Burgi, D. P. Geerke, T. N. Heinz, M. A. Kastenholz, V. Kräutler, C. Oostenbrink, C. Peter, D. Trzesniak, W. F. van Gunsteren, *J. Comput. Chem*. **2005**, *26*, 1719-1751.

[18] T. M. G. Koning, R. Boelens, R. Kaptein, *J. Magn. Res.* **1990**, *90*, 111-123.

[19] X. Daura, K. Gademann, B. Jaun, D. Seebach, W. F. van Gunsteren, A. E. Mark, *Angew. Chem.* **1999**, *111*, 249-253; *Angew. Chem. Int. Ed.* **1999**, *38*, 236-240.

[20] R. Huey, G. M. Morris, A. J. Olson, D. S. Goodsell, *J. Comput. Chem.* **2007**, *28*, 1145-1152.

[21] D. Heckmann, A. Meyer, L. Marinelli, G. Zahn, R. Stragies, H. Kessler, *Angew. Chem.* **2007**, *119*, 3641-3644; *Angew. Chem. Int. Ed.* **2007**, *46*, 3571-3574.

[22] H. B. Schiller, A. Szekeres, B. R. Binder, H. Stockinger, V. Leksa, *Mol. Biol. Cell* **2009**, *20*, 745-56.